HHS Public Access

Author manuscript

Br J Pharmacol. Author manuscript; available in PMC 2022 December 01.

Published in final edited form as:

Br J Pharmacol. 2021 December ; 178(23): 4675–4690. doi:10.1111/bph.15646.

A role for translational regulation by S6 kinase and a downstream target in inflammatory pain

June Bryan de la Peña[1], **Nikesh Kunder**[1], **Tzu-Fang Lou**[1], **Rebecca Chase**[1], **Alexander Stanowick**[1], **Paulino Barragan-Iglesias**[2,3], **Joseph J. Pancrazio**[4,5], **Zachary T. Campbell**[1,5]

[1]Department of Biological Sciences, University of Texas at Dallas, Richardson, Texas, USA

[2]School of Behavioral and Brain Sciences, University of Texas at Dallas, Richardson, Texas, USA

[3]Department of Physiology and Pharmacology, Center for Basic Sciences, Autonomous University of Aguascalientes, Aguascalientes, Mexico

[4]Department of Bioengineering, University of Texas at Dallas, Richardson, Texas, USA

[5]Center for Advanced Pain Studies, University of Texas at Dallas, Richardson, Texas, USA

Abstract

Background and Purpose: Translational controls pervade neurobiology. Nociceptors play an integral role in the detection and propagation of pain signals. Nociceptors can undergo persistent changes in their intrinsic excitability. Pharmacological disruption of nascent protein synthesis diminishes acute and chronic forms of pain-associated behaviours. However, the targets of translational controls that facilitate plasticity in nociceptors are unclear.

Experimental Approach: We used ribosome profiling to probe the translational landscape in dorsal root ganglion (DRG) neurons from male Swiss-Webster mice, after treatment with nerve growth factor and IL-6. Expression dynamics of c-Fos were followed with immunoblotting and immunohistochemistry. The involvement of ribosomal protein S6 kinase 1 (S6K1), a downstream component of mTOR signalling, in the control of c-Fos levels was assessed with low MW inhibitors of S6K1 (DG2) or c-Fos (T-5224), studying their effects on nociceptor activity in vitro using multielectrode arrays (MEAs) and pain behaviour in vivo in Swiss-Webster mice using the hyperalgesic priming model.

Correspondence Zachary T. Campbell, Department of Biological Sciences, University of Texas at Dallas, 800 W. Campbell Road, RL10 BSB 12.510, Richardson, TX 75080, USA. zachary.campbell@utdallas.edu.

AUTHOR CONTRIBUTIONS

Z.T.C., J.J.P., P.B.I. and J.B.D.P. conceived the study. J.B.D.P., P.B.I., T.F.L., N.K. and R.C. performed the experiments. J.B.D.P., P.B.I., T.F.L., N.K., R.C. and A.S. analysed the data. J.B.D.P., N.K., P.B.I., R.C. and Z.C. built the figures. Z.C. and J.B.D.P. wrote the manuscript. All authors approved the manuscript.

CONFLICT OF INTEREST

The authors declare no competing interests.

DECLARATION OF TRANSPARENCY AND SCIENTIFIC RIGOUR

This Declaration acknowledges that this paper adheres to the principles for transparent reporting and scientific rigour of preclinical research as stated in the *BJP* guidelines for Design & Analysis, Immunoblotting and Immunochemistry, and Animal Experimentation, and as recommended by funding agencies, publishers and other organizations engaged with supporting research.

SUPPORTING INFORMATION

Additional supporting information may be found in the online version of the article at the publisher's website.

Key Results: c-Fos was expressed in sensory neurons. Inflammatory mediators that promote pain in both humans and rodents promote c-Fos translation. The mTOR effector S6K1 is essential for c-Fos biosynthesis. Inhibition of S6K1 or c-Fos with low MW compounds diminished mechanical and thermal hypersensitivity in response to inflammatory cues. Additionally, both inhibitors reduced evoked nociceptor activity.

Conclusion and implications: Our data show a novel role of S6K1 in modulating the rapid response to inflammatory mediators, with c-Fos being one key downstream target. Targeting the S6 kinase pathway or c-Fos is an exciting new avenue for pain-modulating compounds.

Keywords

c-Fos; DG2; nociceptor plasticity; pain; S6K; T-5224; translational control

1 | INTRODUCTION

Translation is meticulously controlled. The m^7G cap found ubiquitously on mRNA is bound by the eukaryotic initiation factor 4E (eIF4E) (Yanagiya et al., 2012). eIF4E initiates translation initiation through the recruitment of the scaffolding protein eIF4G and the helicase eIF4A. This protein complex, termed eIF4F, interacts with the Poly(A)-binding protein to stimulate the recruitment of the small ribosomal subunit. eIF4E is the least abundant component of the eIF4F complex and is subject to multifaceted levels of post-translational regulation. For example, the mammalian target of rapamycin (mTOR) kinase phosphorylates and inactivates eIF4E-binding proteins (4EBPs) (Alain et al., 2012). 4EBPs bind to eIF4E, leading to its sequestration. Phosphorylation by mTOR results in increased eIF4E availability and promotes activity-dependent translation. mTOR controls additional factors that govern translation, notably the S6 kinases (S6Ks).

S6K1 and S6K2 are key effectors of mTORC1. They control numerous factors including eukaryotic elongation factor 2 kinase (eEF2K), the ribosomal protein S6, eukaryotic initiation factor 4B (eIF4B) and insulin receptor substrate 1 (IRS-1). eIF4B stimulates the helicase activity of eukaryotic initiation factor 4A (eIF4A) and plays a key role in initiation by recruiting of the small ribosomal subunit to mRNA (Sonenberg & Hinnebusch, 2009). eEF2K controls translation elongation as it phosphorylates and inactivates eukaryotic elongation factor 2 (eEF2) (Browne & Proud, 2002; Ryazanov et al., 1988). S6 is a component of the 40S ribosome and is rapidly phosphorylated in response to mitogens, translational inhibition and nutrient availability (Gressner & Wool, 1974; Krieg et al., 1988; Ruvinsky & Meyuhas, 2006; Wool et al., 1995). S6 was the first S6K target to be identified and is commonly used as a marker for mTOR activity (Knight et al., 2012; Mahoney et al., 2009; Meyuhas, 2015). S6 phosphorylation is increased in the hippocampus during long-term potentiation (Antion, Merhav, et al., 2008). Additionally, application of the $mGlu_1$ receptor agonist dihydroxyphenylhydrazine (DHPG) to hippocampal slices increases S6 phosphorylation (Antion, Hou, et al., 2008). However, the role of S6Ks in pain is far less clear. Genetic ablation of S6Ks throughout development results in increased mechanical sensitivity under baseline conditions (Melemedjian et al., 2013). Rapamycin analogues that target mTORC1 are thought to drive pain through an IRS-1-mediated stimulation of the extracellular signal-regulated kinases (ERK). A major goal of the current work is clarifying

the role of S6Ks in preferential translation in dorsal root ganglion (DRG) neurons and in nociceptive behavioural responses following acute inhibition in adult animals.

Noxious cues that promote pain in humans and rodents can affect translation (Melemedjian et al., 2010). For example, the cytokine IL-6 activates mitogen-activated protein kinase (MAPK)-interacting kinases (MNK1/2 referred to as MNKs), increasing eIF4E phosphorylation (Melemedjian et al., 2010; Melemedjian et al., 2014). Inhibition of MNKs with cercosporamide or genetic elimination of eIF4E phosphorylation attenuates mechanical hypersensitivity evoked by IL-6 (Moy et al., 2017). Similarly, a blockade of MNKs with eFT-508 interferes with the sensitization of nociceptors by IL-6 (Jeevakumar et al., 2020). A second inflammatory mediator, nerve growth factor (NGF), stimulates mTOR and increases nascent protein synthesis (Melemedjian et al., 2010). Both inflammatory mediators produce long-lasting hyperalgesia (Dina et al., 2008; Lewin et al., 1994; Oka et al., 1995; Rukwied et al., 2010). Neutralization of either NGF or IL-6 is therapeutically useful in humans (Cattaneo, 2010; Nishimoto et al., 2009). A broad array of protein synthesis inhibitors that target translation initiation disrupts hyperalgesic priming by NGF and IL-6 (Barragan-Iglesias et al., 2018; Melemedjian et al., 2010; Moy et al., 2017). Only now is the repertoire of mRNAs subject to selective translation becoming clear. Much work remains to be done in order to understand how batteries of transcripts are subject to coordinate control on a post-transcriptional basis and how these controls contribute to pain.

Immediate-early genes (IEGs) are rapidly induced in response to a range of stimuli, including neuronal activity (Minatohara et al., 2015). IEGs serve critical roles in bridging extracellular stimuli to intracellular responses (Morgan & Curran, 1991) and a prime example of these IEGs is c-Fos. It was among the first transcription factors identified as being responsive to neuronal activity (Hunt et al., 1987; Morgan et al., 1987; Sagar et al., 1988). Mechanistically, c-Fos forms heterodimers with Jun to generate the AP-1 transcription factor (Chiu et al., 1988). cAMP and Ca^{2+} stimulate c-Fos production potentially through activation of CREB (Gandolfi et al., 2017). c-Fos is used as a marker of neuronal activity in a wide range of contexts. For example, in one class of GABAergic interneuron in the olfactory system, odours promote c-Fos expression in an mTOR-dependent manner (Liu et al., 2018). c-Fos is induced by neuronal activity in the CNS (Sagar et al., 1988). Furthermore, an array of noxious cues promotes c-Fos expression in the spinal cord (Avelino et al., 1997; Buritova et al., 1997; Hunt et al., 1987). c-Fos has been detected in nociceptors and is thought to be selectively imported into the nucleus in support of neuropathic pain (Marvaldi et al., 2020). Yet the mechanisms that govern c-Fos production in DRG neurons remain unclear.

We previously applied ribosome profiling to DRG neurons isolated from adult mice (Barragan-Iglesias et al., 2020). We examined translation 20 min after the addition of NGF and IL-6. We identified just over 200 mRNAs that display an increase in translation. Here, we have examined the mechanistic basis of the increases in translation triggered by inflammatory mediators. We found that S6 phosphorylation was induced by NGF and IL-6 contemporaneously with the translation of c-Fos. Blockade of S6K1 with the low MW inhibitor DG2 (Okuzumi et al., 2009) prevented induced translation of c-Fos and nociceptor sensitization. In parallel, we examined the effects of c-Fos inhibition on

nociceptor excitability. Blockade of c-Fos by T-52224 (Makino et al., 2017) diminished excitability by NGF and IL-6 in vitro. Lastly, we demonstrated that inhibition of either S6K1 or c-Fos attenuated mechanical and thermal sensitivity induced by NGF and IL-6 in vivo.

2 | METHODS

2.1 | Animals

All animal care and experimental procedures were approved by the Institutional Animal Care and Use Committee at The University of Texas at Dallas and were in accordance with International Association for the Study of Pain guidelines. Animal studies are reported in compliance with the ARRIVE guidelines (Percie du Sert et al., 2020) and with the recommendations made by the *British Journal of Pharmacology* (Lilley et al., 2020).

Male Swiss Webster (SW) mice (IMSR Cat# TAC:sw, RRID: IMSR_TAC:sw), purchased from Taconic Bioscience, were used for both in vitro primary DRG cultures and in vivo behavioural experiments. Animals were housed in a humidity- and temperature-controlled vivarium with a 12-h light/dark cycle, with food and water available ad libitum.

2.2 | Primary DRG culture

DRGs (C1-L5) from 4- to 6-week-old SW mice were harvested and stored in chilled Hanks' balanced salt solution (HBSS; Invitrogen). DRGs were enzymatically dissociated with collagenase A (1 mg·ml^{-1}, Roche) for 25 min and collagenase D (1 mg·ml^{-1}, Roche) with papain (30 U·ml^{-1}, Roche) for 20 min at 37°C. DRGs were then triturated in a 1:1 mixture of 1-mg·ml^{-1} trypsin inhibitor (Roche) and bovine serum albumin (BSA) (Thermo Fisher Scientific) and then filtered through a 70-μm cell strainer (Corning). Cells were pelleted and then resuspended in DRG culture media: DMEM/F12 with GlutaMAX (Thermo Fisher Scientific) containing 10% fetal bovine serum (FBS; Thermo Fisher Scientific), 1% penicillin and streptomycin and 3-μg·ml^{-1} 5-fluorouridine with 7-μg·ml^{-1} uridine to inhibit mitosis of non-neuronal cells. Cells were plated according to the downstream application.

2.3 | Ribosome profiling

DRG culture, library generation and sequencing were carried out as described previously (Barragan-Iglesias et al., 2020). Briefly, DRG cultures from 10 SW mice per replicate were treated with mouse NGF (20 ng·ml^{-1}) and recombinant mouse IL-6 (50 ng·ml^{-1}) for 20 min, followed by emetine (50 μg·ml^{-1}) and then lysed with a polysome lysis buffer. Ribosome-bound RNAs were isolated by MicroSpin S-400 columns (GE Healthcare), rRNA contaminants were removed using RiboCop rRNA depletion kit (Lexogen) and ribosome footprints were size selected (28–34 nt) by PAGE (Bio-Rad). Footprints were generated by SMARTer smRNA-Seq kit for Illumina (TaKaRa). RNA abundance was quantified using the Quantseq 3′ mRNA-Seq library kit (Lexogen). The concentrations of purified libraries were quantified using Qubit (Invitrogen), and the average size was determined by fragment analyser with high-sensitivity normal goat serum (NGS) fragment analysis kit (Advanced Analytical Technologies Inc.). Libraries were then sequenced on an Illumina NextSeq500 sequencer using 75-bp single-end high-output reagents (Illumina).

Sequencing data were subjected to quality check using FastQC 0.11.5 (Babraham Bioinformatics, RRID:SCR_014583). Adapters were subjected to trimming based on adapter sequences. Mapping was conducted with TopHat 2.1.1 (RRID:SCR_013035) with Bowtie 2.2.9 (RRID:SCR_005476) to the mouse reference genome (NCBI reference assembly GRCm38.p4) and reference transcriptome (Gencode vM10, RRID:SCR_014966). Strand orientation was considered during the mapping process. Processed bam files were quantified for each gene using Cufflinks 2.2.1 (RRID:SCR_014597) with gencode.vM10 genome annotation. Read counts were not normalized by length by using the Cufflinks option—no–length–correction. Relative abundance for the ith gene was determined by calculating TPM (transcripts per million) values. Finally, TPM values were normalized to the upper decile for each biological replicate, and udTPM (upper decile TPM) was used for analysis to provide uniform processing for samples with varying sequencing depth.

2.4 | Single-cell data

Single-cell DRG sequencing data were generated based on published data (Usoskin et al., 2015). For visualization, we used the Seurat package 2.2.1 (RRID:SCR_007322) (Butler et al., 2018; Linderman & Steinerberger, 2019).

2.5 | Immunohistochemistry

DRG (L3-L5) sections were fixed in ice-cold 4% paraformaldehyde (PFA) in 1× TBS for 1 h and then subsequently washed three times for 5 min each in 1× TBS. Slides were then incubated in a permeabilization solution made of TBS with 0.4% Triton X-100 (Sigma-Aldrich) for 30 min and then were washed three times with TBS. Tissues were blocked for at least 2 h in 10% NGS (Atlanta Biologicals, Atlanta, GA, USA) and 1% BSA (Thermo Fisher Scientific) in TBS. Primary antibodies against c-Fos (1:20; Sigma, cat. # PC05, RRID:AB_564450), peripherin (1:1000; Novus, cat. # NBP1-05423, RRID:AB_1556333) and NeuN (1:1000; Synaptic Systems, cat. # 266 004, RRID:AB_2619988) were incubated overnight at 4°C. The next day, slides were washed with TBS, and then, appropriate secondary antibodies (Alexa Fluor, Invitrogen) were applied for 2 h. After additional washes, coverslips were mounted on slides with ProLong Gold antifade mountant (Invitrogen).

2.6 | Immunocytochemistry

DRGs were cultured as described above and plated in eight-well chamber slides (Nunc Lab-Tek, Thermo Fisher Scientific). Cultures were fixed in ice-cold 4% PFA in 1× PBS for 20 min and then washed with PBS three times for 5 min each time. Cells were then permeabilized with 0.025% Triton X-100 (Sigma) in PBS containing 1% BSA for 30 min. After washes, slides were blocked by 10% NGS and 1% BSA in PBS for at least 1 h. Primary antibodies were used to detect the following proteins: c-Fos (1:20; Sigma, cat. # PC05, RRID:AB_564450), phospho-S6 ($S^{235/236}$) (1:100; Cell Signaling Technology [CST], cat. # 4858, RRID:AB_916156), phospho-S6 ($S^{240/244}$) (1:800; CST, cat. # 5364, RRID:AB_10694233), S6 ribosomal protein (1:200: CST, cat. # 2217, RRID:AB_331355) and peripherin (1:1000; Novus, cat. # NBP1-05423, RRID:AB_1556333). Primary antibodies were incubated at 4°C overnight. The next day,

appropriate secondary antibodies (Alexa Fluor, Invitrogen) were applied for 1 h. Following additional PBS washes, coverslips were mounted with ProLong Gold.

2.7 | Image acquisition and analysis

All images were acquired using an FV-3000RS confocal microscope (Olympus). Immunohistochemistry (IHC) colocalization of c-Fos to peripherin and NeuN was calculated using ImageJ (RRID:SCR_003070) plug-in, JACoP, and represented as % of c-Fos-positive cells expressing markers (Bolte & Cordelières, 2006). Immunocytochemistry (ICC) images were quantified using the corrected total cell fluorescence (CTCF) method with the following formula: CTCF = Integrated density − (Area of selected cell × Mean fluorescence of background readings). To quantify cellular localization of c-Fos, DAPI and peripherin were used to identify the nucleus and cytoplasm, respectively. CTCF was then used to measure c-Fos signal intensity.

2.8 | Protein immunoblotting

Primary DRGs from five mice were evenly distributed in a six-well plate coated with poly-D-lysine and maintained at 37°C in a humidified 95% air/5% CO_2 incubator with fresh culture media replacement every other day. At 6 days in vitro (DIV), cells were treated with NGF (20 ng·ml^{-1}) and IL-6 (50 ng·ml^{-1}) for 20, 60 and 120 min. Cells were rinsed with chilled PBS then lysed in lysis buffer (50 mM Tris, pH 7.4, 150 mM NaCl, 1 mM EDTA, pH 8.0 and 1% Triton X-100) containing protease and phosphatase inhibitors (Sigma-Aldrich). Total protein was extracted by ultrasonication, and the supernatant was collected by centrifugation at 18,000 × *g* for 20 min at 4°C. Protein concentration was quantified using Pierce B.C.A. protein assay kit (Thermo Fisher Scientific). For each sample, 20 μg of protein in Laemmli buffer (Bio-Rad) was loaded and separated by 10% SDS-PAGE gels and then transferred to Immobilon-P membranes (Millipore). Membranes were washed in TBS with 0.05% Tween-20 (TBS-T) and blocked with 5% low-fat milk for 1 h at room temperature. Primary antibodies were used to detect the following proteins: c-Fos (1:1000, CST, cat. # 2250), phospho-S6 ($S^{235/236}$) (1:1000; CST, cat. # 4858), phospho-S6 ($S^{240/244}$) (1:1000; CST, cat. # 5364), S6 ribosomal protein (1:1000: CST, cat. # 2217) and GAPDH (1:10,000, CST, cat # 2118). Primary antibodies were incubated overnight at 4°C with gentle agitation. After primary incubation, membranes were washed with TBS-T (3 × 10 min each wash) and incubated with appropriate secondary antibodies conjugated to horseradish peroxidase (Jackson ImmunoResearch) for 1 h at room temperature. Following washes, the signal was detected using Western Chemiluminescent HRP Substrate (ECL) (MilliporeSigma) on ChemiDoc Touch Imaging System (Bio-Rad). Analysis was performed using Image Lab 6.0.1 (Bio-Rad). Phosphorylated S6 ribosomal proteins were normalized to their respective total protein, whereas c-Fos was normalized to GAPDH. Data are expressed as a percent of change compared with vehicle groups.

2.9 | Mechanical and thermal behavioural testing

Hyperalgesic priming was induced by intraplantar (i.pl.) injection of NGF (50 ng) and IL-6 (1.25 ng) in 25-μl saline into the right hind paw of mice. To measure mechanical sensitivity, we used calibrated von Frey filaments (Stoelting, Wood Dale, IL, USA). Mice were placed in acrylic boxes with wire mesh floors and allowed to habituate for 1 h. Then, von Frey

filaments were applied to the plantar surface of the hind paw of mice for 1–3 s, and the up–down method was used to calculate the mechanical withdrawal threshold in grams (g). Measurements were made at various time points after NGF and IL-6 administration. When animals returned to their original baseline thresholds at Day 9, priming was examined by i.pl. injection of a subthreshold dose of PGE_2 (100 ng), and the mechanical sensitivity was again assessed at 3 and 24 h post-PGE_2 administration.

To measure thermal sensitivity, we used the Hargreaves test to determine the paw withdrawal latency in response to a focused, radiant heat light source (Hargreaves et al., 1988). Mice were placed on a glass floor, and a focused beam of high-intensity light was aimed at the plantar surface of the hind paw. The light intensity was set to 40% following manufacturer instructions (IITC Model 390) with a cut-off value of 20 s. Withdrawal latency measurements were taken in triplicate, with each trial being separated by at least 10 min, to decrease experimental variability. After determining baseline withdrawal thresholds, thermal hypersensitivity was evaluated 1 and 24 h after NGF and IL-6 treatment.

DG2 or T-5224 was co-administered with NGF and IL-6. The doses used were based on previous studies or pilot experiments (Marvaldi et al., 2020). All assignments of treatments and the measurements were fully randomized. All behavioural observations were made by experienced experimenters who were blinded to the experimental conditions.

2.10 | MEA culture, recordings and analysis

Multielectrode array (MEA) experiments were performed as described previously with minor modifications (Barragan-Iglesias et al., 2021). Briefly, DRG neurons were seeded on 48-well MEA plates (Axion Biosystems, USA) which had been coated with 0.1% PEI and 20-$\mu g \cdot ml^{-1}$ laminin at 30,000 neurons per well. Wells were filled with 300 µl of DRG culture medium supplemented with 5-$ng \cdot ml^{-1}$ GDNF. DRGMEA cultures were maintained in cell culture incubators at 37°C, 5% CO_2 and 95% humidity.

Spontaneous and evoked extracellular recordings were carried out using an Axion Maestro recording system (Axion Biosystems, USA). Filtered continuous recordings were collected from all 48 wells (768 total electrodes) simultaneously at a 12.5-kHz sampling rate. Extracellular spikes were defined as filtered continuous data crossing an adaptive threshold of $\pm 5.5\sigma$ based on 1-s snapshots of root mean square (RMS) noise. Active electrodes were defined as those exhibiting a minimum of one spike per minute during baseline spontaneous extracellular recordings and were used in further analyses. Spontaneous neuronal activity was recorded every alternate day beginning at DIV 5 to confirm viable culture conditions and to detect stable spontaneous baselines. MEA recordings were carried out between DIV 9 and 15 on cultures exhibiting at least one spontaneously active electrode per well. Environmental conditions (37°C, 5% CO_2 and 95% humidity) were maintained throughout the recording duration.

A 30-min baseline recording was taken before the addition of any compounds. Only wells with spontaneously active electrodes were used for further experiments. Compounds were administered to wells, and the plate was immediately taken back to the Axion recording system, where they were first acclimated for 10 min then followed by a 30-min recording

period. We had the following treatment groups: vehicle, NGF (20 ng·ml^{-1})/IL-6 (50 ng·ml^{-1}), NGF/IL-6 with DG2 (2, 20 and 200 μM) or NGF/IL-6 with T-5224 (1, 10 and 100 μM). Doses used were based on previous studies or pilot experiments. Mean firing rates (MFRs) of each group were normalized to its baseline firing rate (treatment MFR/combined baseline MFR) and presented as relative to the vehicle group.

2.11 | Data and statistical analysis

The data and statistical analysis comply with the recommendations on experimental design and analysis in pharmacology (Curtis et al., 2018). Data are presented as mean ± SEM of at least six animals per group. The sample size was estimated as $n = 6$ using G*power (RRID:SCR_013726) for a power calculation with 80% power, expectations of 50% effect size, with α set to 0.05. Exact numbers of samples per group are shown in the Figure legends. GraphPad Prism Version 9.0 (GraphPad Software, RRID: SCR_002798) was used for graph plotting and statistical analysis. The Student's t test was used to compare two independent groups. Statistical evaluation for three or more separate groups was performed by one-way or two-way analysis of variance (ANOVA), followed by Sidak's multiple comparison test, and the a priori level of significance at 95% confidence level was considered at $P < 0.05$. Appropriate diagnostic statistics were carried out to ensure valid use of parametric statistics. Specific statistical tests used are described in the Figure legends.

2.12 | Materials

DG2 and mouse NGF was supplied by Millipore-Sigma (Burlington, MA, USA); T-5224 and PGE_2 by Cayman Chemicals (Ann Arbor, MI, USA). The recombinant mouse IL-6 was supplied by R&D Systems (Minneapolis, MN, USA).

2.13 | Nomenclature of targets and ligands

Key protein targets and ligands in this article are hyperlinked to corresponding entries in, the IUPHAR/BPS Guide to PHARMACOLOGY (http://www.guidetopharmacology.org) and are permanently archived in the Concise Guide to PHARMACOLOGY 2019/20 (Alexander et al., 2019).

3 | RESULTS

3.1 | Ribosome profiling reveals c-Fos as a target of preferential translation

We previously conducted ribosome profiling and RNA sequencing on cultured DRG neurons subjected to either a vehicle or plasticity treatment consisting of a combination of NGF and IL-6 for 20 min (Figure 1a) (Barragan-Iglesias et al., 2020). Among transcripts with the largest significant increase in translation was the IEG and transcription factor, c-Fos (Figure 1b, adjusted fold change = 1.91). Under baseline conditions, c-Fos is readily detected (Figure 1c). The addition of NGF and IL-6 resulted in rapid translation of c-Fos as judged by accumulation of ribosome protected footprints. However, the levels of the c-Fos transcript were not significantly altered (Barragan-Iglesias et al., 2020). This result led us to hypothesize that translational regulation may facilitate c-Fos biosynthesis.

3.2 | c-Fos is expressed in DRG neurons

Next, we sought to characterize the expression of c-Fos in the DRG. We examined previously reported single-cell sequencing data (Usoskin et al., 2015). Cells were divided into clusters based on principal component analysis. We defined clusters based on the expression of the following marker genes: *Vim* (non-neuronal), *Calca* (peptidergic), *Mrgprd* (non-peptidergic), *Th* (tyrosine hydroxylase) and *Nefh* (large-diameter neurons) (Figure 2a). Based on the relative expression of c-Fos across these groups, we found that it is ubiquitously present in neurons (29%) and non-neurons (31%). Within the neuronal population, c-Fos is broadly expressed in each neuronal subtype: peptidergic (14%), non-peptidergic (25%), TH-positive (30%) and neurofilament (36%) (Figure 2a,b).

To test the prediction that DRG neurons express c-Fos, we conducted IHC on DRG tissues isolated from wild-type mice. It is of note that whereas NeuN is a pan-neuronal marker, peripherin is a marker for small- and medium-diameter neurons, which are mostly nociceptors (Ferri et al., 1990). We found that c-Fos is readily detected in cells that express the neuronal markers NeuN (90.52%) and peripherin (73%) (Figure 2c,d). To examine the subcellular localization of c-Fos, we conducted ICC on peripherin-positive DRG neurons. We found that c-Fos is predominantly present in the cytoplasm. The addition of NGF and IL-6 resulted in a modest increase in c-Fos levels (Figure 2e,f) and changed its cellular distribution becoming more localized in the nucleus (Figure 2e,g). This result resembles the recent finding that c-Fos is transported to the nucleus after nerve injury (Marvaldi et al., 2020). Collectively, our results indicate that c-Fos is present in DRG neurons and that its expression profile changes after NGF/IL-6 treatment.

3.3 | S6K1 mediates translation of c-Fos

We next asked how c-Fos levels are controlled in DRG neurons. As mTOR activity is stimulated by NGF and, to a lesser extent, by IL-6, we reasoned that the activity of S6K1 would be elevated (Melemedjian et al., 2010). We examined S6 phosphorylation using immunoblots over a 2-h period following the addition of NGF and IL-6 (Figure 3a). We found that phosphorylation of S6 at the $S^{235/236}$ position was increased by approximately 175%, whereas total S6 levels were unchanged (Figures 3a). Importantly, phosphorylation was attenuated by the S6K1 inhibitor DG2 (Figure 3a). As an additional test, we conducted ICC and examined the same sites of phosphorylation. Phosphorylation of S6 at amino acids 235 and 236 was increased by NGF/IL-6 treatment and this was again abolished by co-treatment with DG2 (Figure 3b). We next probed S6 phosphorylation at a second position ($s^{240/244}$) and observed similar dynamics (Figure 3c). Total S6 levels were unaltered by any of the treatments (Figure 3d). These observations prompted us to inquire as to if S6K activity is required for translational stimulation of c-Fos triggered by NGF and IL-6. We found that DG2 blocked preferential translation of c-Fos after the addition of NGF/IL-6 but importantly had no effect on the production of the GAPDH control (Figures 3e). Collectively, these results reveal that inhibition of S6K1 with DG2 prevents both S6 phosphorylation and preferential translation of c-Fos in DRG neurons.

3.4 | Pharmacological inhibition of S6K1 or c-Fos blocks NGF/IL-6-induced neuronal firing and behavioural hypersensitivity

Does c-Fos or the S6K pathway contribute to plasticity in nociceptors? We approached this problem initially by measuring nociceptor activity in vitro. We asked if antagonism of S6K1 by DG2 or of c-Fos by the low MW inhibitor T-5224 would reduce evoked activity of DRG neurons. Extracellular recordings of cultured DRG neurons were obtained using MEAs (Figure 4a) (Black et al., 2018; Black et al., 2019). In these devices, DRG neurons are cultured within microfabricated wells with substrated integrated electrode sites capable of detecting action potentials extracellularly. We asked if addition of NGF and IL-6 enhances spontaneous firing rates. In fact, the MFR was increased by over twofold (Figure 4b). We next asked if evoked firing was affected by co-treatment with DG2 (2, 20 and 200 μM). Indeed, we found that DG2 at 20 μM diminished evoked firing rates (Figure 4b,c). We tested the effects of c-Fos inhibition on evoked activity using three concentrations of T-5224 (1, 10 and 100 μM) and found that T-5224 resulted in baseline levels of activity at each of the concentrations used (Figure 4b,d). A caveat to these measurements is that they were conducted in the presence of GDNF which enhances c-Fos expression (He et al., 2008). This is necessary because GDNF promotes maturation of the cultures. Collectively, the data suggest that S6Ks contribute to the enhanced firing and that c-Fos may play a key role in sensitization.

One assay to quantify allodynia is the measurement of mechanical withdrawal thresholds following the application of calibrated von Frey filaments (Aley et al., 2000; Reichling & Levine, 2009). At baseline, mice display a threshold of approximately 1.0–1.5 g before a reflexive withdrawal. Intraplantar injection of inflammatory mediators such as NGF and IL-6 causes sensitization in nociceptors and increased sensitivity to mechanical stimulation. Co-injection of drugs enables reliable assays of analgesia (an increase in threshold) or hyperalgesia (a decrease in threshold). After the resolution of an initial insult, we inject a second subthreshold dose (100 ng) of PGE_2. In a naïve animal, this relatively low dose of PGE_2 does not result in long-term sensitivity. However, in primed animals, PGE2 evokes long-lasting allodynia. This model, termed hyperalgesic priming, is thought to model the transition from acute to chronic pain (Reichling & Levine, 2009).

We first asked if S6Ks are required for the acute phase of mechanical sensitivity at either a low (100 ng) or high (600 ng) dose of DG2 (Figure 5a) and found that the low dose displayed similar sensitivity to the vehicle-treated control. However, the high dose led to a significant decrease in mechanical allodynia from 6 h to 3 days prior to returning to baseline. We next asked if priming was disrupted by DG2 following injection of PGE_2 on Day 9 (Figure 5b). Indeed, for the high-dose group, we found that priming was diminished. Given the effects of the high-dose DG2 on mechanical sensitivity, we also tested its effects on thermal sensitivity, by measuring thermal withdrawal latency using the Hargreaves method (Figure 5c). We found a small but significant antinociceptive effect from the high dose of DG2 at the 1-h time point. This effect was absent after 24 h.

Next, we examined the effects of the c-Fos inhibitor T-5224 on mechanical sensitivity (Figure 5d), using the same method. Both the low dose (300 ng) and the high dose (3 μg) of T-5224 reduced allodynia between 6 h and 6 days. The high dose also had a significant

effect at 1 h that was not evident at the lower dose. Both doses prevented priming at 24 h but did not have an effect at the 1-h time point (Figure 5e). Finally, we tested the effect of T-5224 on thermal sensitivity and found that the high dose reduced thermal sensitivity at the 1-h time point (Figure 5f). Collectively, our results suggest that pharmacological inhibition of S6Ks or c-Fos diminished pain-associated behaviours in mice.

4 | DISCUSSION

Our data enable us to make three major conclusions. First, translation of an IEG is mediated by S6K1 in DRG neurons. Second, S6K1 contributes to sensitization and inflammatory pain. Third and finally, the transcription factor c-Fos is similarly important to evoked nociceptor activity and behaviours associated with pain in response to inflammatory mediators. We discuss the implications of each of our finding in turn.

To date, we have identified two IEGs that are rapidly induced in DRG neurons in response to NGF and IL-6, Arc and c-Fos. In prior work, Arc was rapidly translated in vitro and locally translated in glabrous skin in vivo (Barragan-Iglesias et al., 2020). Mice that lack Arc display little to no change in nociceptive responses, despite changes in vasodilation (Barragan-Iglesias et al., 2020; Hossaini et al., 2010). This prompted us to ask if other transcripts subject to induced translation were involved in nociception. A key question is how the several hundred mRNAs, including c-Fos, identified in our ribosome profiling study are co-ordinated on a translational basis, in response to extracellular cues (Barragan-Iglesias et al., 2020). We focused on S6K1 in part because stimuli that trigger S6 phosphorylation also trigger the local translation of Arc in the CNS (Pirbhoy et al., 2016) and found that translation of c-Fos requires S6K1 activity. We also found that Arc translation is lost upon inhibition of S6Ks in DRG neurons (unpublished observation). Collectively, this suggests that S6K1 activity is broadly important for the production of IEGs in DRG neurons.

How does S6K1 target subsets of the transcriptome? There are multiple non-mutually exclusive possibilities. First, eEF2K is downstream of S6Ks and its activity has been linked to Arc biosynthesis (Park et al., 2008). eEF2K targets a single protein, eEF2, and represses its activity. It is clear that repression by eEF2K affects only a subset of the transcriptome (Kenney et al., 2016). Intriguingly, behavioural deficits in FMRP-deficient mice are rescued upon genetic removal of S6K1 (Bhattacharya et al., 2012). Ribosome profiling analyses suggest that length-dependent decreases in translation elongation in FMRP animals are rescued upon loss of S6K1 (Bohlen & Teleman, 2021). Thus, translation elongation may be a critical function of S6K signalling. A second possibility is that S6Ks act on eIF4B. eIF4B stimulates the helicase function of eIF4A (Andreou et al., 2017). However, the consequences of eIF4B phosphorylation on translation are unclear (Gingras et al., 2001). Third and finally, S6Ks and mTOR signalling have also been linked to upstream open reading frames (uORF; Schepetilnikov et al., 2013). uORF translation typically diminishes initiation at downstream start sites. However, activation of S6Ks appears to promote re-initiation. Given that a uORF has been linked to nociception, this is an interesting possibility (Barragan-Iglesias et al., 2021).

The mTOR signalling axis permeates plasticity. Although effects on the availability and activity of eIF4E have attracted significant attention, it is less clear if other factors play significant roles in pain-associated plasticity (Megat et al., 2019; Moy et al., 2017; Sarah Loerch et al., 2019). We found that inhibition of S6K1 diminishes evoked excitability. A prior study found that an S6K1 inhibitor, PF-4708671, resulted in mechanical allodynia (Melemedjian et al., 2013). This was observed after 3 days of systemic dosing at 50 $mg \cdot kg^{-1}$ and may not have been a neuronally mediated effect. Additionally, this was one of the first S6K1 inhibitors to be discovered and has a 50% inhibitory concentration of 160 nM (Pearce et al., 2010). In addition to delivering a much lower dose directly into the paw, DG2 is much more potent and has an IC_{50} value of 9.1 nM (Bhatt et al., 2016; Okuzumi et al., 2009). Our data provide proof of concept that local disruption of S6K1 may provide a viable strategy for targeting inflammatory pain and establishes a rationale for probing the role of S6Ks in other pain states.

We identified c-Fos as a key player in sensitization and pain amplification (Figure 6). It is notable that our study was conducted in males. A lingering question is if this mechanism is shared in females. Additionally, a paramount question is if the effects we observe are entirely neuronally mediated. c-Fos expression is not confined to neurons, and it has been used as a marker of injury in the spinal cord (Avelino et al., 1997; Buritova et al., 1997; Hunt et al., 1987). c-Fos also plays key roles in the immune system. Inhibition of c-Fos attenuates collagen-induced arthritis by preventing the production of matrix-degrading metalloproteases (MMPs) and inflammatory cytokines (Aikawa et al., 2008). Members of each group are prominent in neuropathic pain. Thus, we cannot discount the possibility that non-neuronal cells also contribute to the behavioural effects we observed. A potential caveat to the behavioural experiments is that the c-Fos inhibitor (T-5224) was injected into the paw. Given that c-Fos is understood largely as a transcription factor, a parsimonious explanation is that c-Fos inhibition in non-neuronal cells could be the mechanism underlying allodynia. Alternatively, administration of transcriptional inhibitors appears to affect transcription at distal sites. For example, injection of double-stranded oligonucleotides that mimic the consensus binding element of the neuronal transcription factor CREB in the paw diminished pain in an IL-6 priming model (Melemedjian et al., 2014). The finding that evoked firing in neuronal cultures is reduced by a c-Fos inhibitor implies that the compound might act on neurons, given that the vast majority of immune cells are eliminated through the cell isolation procedures. Moreover, the prolonged use of mitotic inhibitors during culture maintenance reduces the abundance of non-neuronal cells. The effects of DG2 and T-5224 during the later phase (1–6 days after NGF/IL-6) and during the PGE_2 priming phase of the hyperalgesic priming model also suggest involvement of nociceptors. c-Fos appears to act specifically in nociceptors as knockdown of c-Fos in nociceptors reduces thermal sensitivity in a neuropathic pain model (Marvaldi et al., 2020). Inhibition of c-Fos by T-5224 attenuated the development and maintenance of neuropathic pain, suggesting that c-Fos is broadly important for pain-associated behaviours. It is possible that S6K1-mediated regulation of c-Fos is the relevant mechanism driving early pain response whereas importin a3-mediated nuclear import of c-Fos is required for chronic pain. Unambiguous identification of the cellular process responsible for the contribution of c-Fos to pain-associated behaviours is

an important problem moving forward and could potentially be addressed through genetic experiments in vivo.

The identification of S6K1 and c-Fos as key regulators in the development of inflammatory pain opens exciting new targets for drug development. The low MW inhibitors DG2 and T-5224 may function as broad-spectrum anti-hyperalgesic agents and this possibility warrants further investigation. Other members of the c-Fos family of transcription factors might also play a role in chronic pain. For instance, the c-Fos homolog FosB promotes long-term adaptive changes in the CNS and has been linked to the production of signalling molecules involved in pain such as dynorphin (Dubner & Ruda, 1992; Zachariou et al., 2006). However, it is unclear precisely what c-Fos targets in the periphery and how distinct networks of gene control differ between members of the c-Fos family in neurons. This work provides a motivation to probe the targets of c-Fos in order to better understand its function within nociceptors.

Supplementary Material

Refer to Web version on PubMed Central for supplementary material.

ACKNOWLEDGEMENTS

This work was supported by National Institutes of Health Grants R01NS100788 (Z.T.C.) and R01NS114018 (Z.T.C.), the PRODEP's Program (P.B.I.), the IBRO Return Home Fellowship (P.B.I.) and the IASP Early Career Research Grant (P.B.I.).

DATA AVAILABILITY STATEMENT

The data that support the findings of this study are available from the corresponding author upon reasonable request. Some data may not be made available because of privacy or ethical restrictions. This article includes all datasets/codes generated or analysed during this study. Sequencing data are available on GEO https://www.ncbi.nlm.nih.gov/geo/query/acc.cgi?acc=GSE117043.

Abbreviations:

DG2	3-Bromo-4-(4-(2-methoxyphenyl)piperazin-1-yl)-1H-pyrazolo[3,4-d]-pyrimidine
DRG	dorsal root ganglion
IEG	immediate early gene
IHC	immunohistochemical
ICC	immunocytochemistry
MEA	multielectrode array
MFR	mean firing rates
mTOR	mammalian target of rapamycin

NGF	nerve growth factor
S6K	S6 kinase
T-5224	5-[4-(cyclopentyloxy)-2-hydroxybenzoyl]-2-[(2,3-dihydro-3-oxo-1,2-benzisoxazol-6-yl)methoxy]-benzenepropanoic acid
uORF	upstream open reading frames

REFERENCES

Aikawa Y, Morimoto K, Yamamoto T, Chaki H, Hashiramoto A, Narita H, Hirono S, & Shiozawa S (2008). Treatment of arthritis with a selective inhibitor of c-Fos/activator protein-1. Nature Biotechnology, 26(7), 817–823. 10.1038/nbt1412

Alain T, Morita M, Fonseca BD, Yanagiya A, Siddiqui N, Bhat M, Zammit D, Marcus V, Metrakos P, Voyer LA, Gandin V, Liu Y, Topisirovic I, & Sonenberg N (2012). eIF4E/4E-BP ratio predicts the efficacy of mTOR targeted therapies. Cancer Research, 72(24), 6468–6476. 10.1158/0008-5472.CAN-12-2395 [PubMed: 23100465]

Alexander SPH, Fabbro D, Kelly E, Mathie A, Peters JA, Veale EL, Armstrong JF, Faccenda E, Harding SD, Pawson AJ, Sharman JL, Southan C, Davies JA, & CGTP Collaborators. (2019). THE CONCISE GUIDE TO PHARMACOLOGY 2019/20: Enzymes. British Journal of Pharmacology, 176, S297–S396. 10.1111/bph.14752 [PubMed: 31710714]

Aley KO, Messing RO, Mochly-Rosen D, & Levine JD (2000). Chronic hypersensitivity for inflammatory nociceptor sensitization mediated by the epsilon isozyme of protein kinase C. The Journal of Neuroscience: The Official Journal of the Society for Neuroscience, 20(12), 4680–4685. 10.1523/JNEUROSCI.20-12-04680.2000 [PubMed: 10844037]

Andreou AZ, Harms U, & Klostermeier D (2017). eIF4B stimulates eIF4A ATPase and unwinding activities by direct interaction through its 7-repeats region. RNA Biology, 14(1), 113–123. 10.1080/15476286.2016.1259782 [PubMed: 27858515]

Antion MD, Hou L, Wong H, Hoeffer CA, & Klann E (2008). mGluR-dependent long-term depression is associated with increased phosphorylation of S6 and synthesis of elongation factor 1A but remains expressed in S6K-deficient mice. Molecular and Cellular Biology, 28(9), 2996–3007. 10.1128/MCB.00201-08 [PubMed: 18316404]

Antion MD, Merhav M, Hoeffer CA, Reis G, Kozma SC, Thomas G, Schuman EM, Rosenblum K, & Klann E (2008). Removal of S6K1 and S6K2 leads to divergent alterations in learning, memory, and synaptic plasticity. Learning & Memory (Cold Spring Harbor, NY), 15(1), 29–38.

Avelino A, Cruz F, & Coimbra A (1997). Sites of renal pain processing in the rat spinal cord. A *c-fos* study using a percutaneous method to perform ureteral obstruction. Journal of the Autonomic Nervous System, 67(1–2), 60–66. 10.1016/S0165-1838(97)00105-7 [PubMed: 9470145]

Barragan-Iglesias P, de la Peña JB, Lou T-F, Loerch S, Kunder N, Shukla T, Basavarajappa L, Song J, Megat S, Moy J, & Wangzhou A Intercellular Arc signaling regulates vasodilation. bio-Rxiv. 2020.

Barragan-Iglesias P, Kunder N, Wanghzou A, Black B, Ray PR, Lou TF, Bryan de la Peña J, Atmaramani R, Shukla T, Pancrazio JJ, Price TJ, & Campbell ZT (2021). A peptide encoded within a 5′ untranslated region promotes pain sensitization in mice. Pain, 162, 1864–1875. 10.1097/j.pain.0000000000002191 [PubMed: 33449506]

Barragan-Iglesias P, Lou TF, Bhat VD, Megat S, Burton MD, Price TJ, & Campbell ZT (2018). Inhibition of Poly(A)-binding protein with a synthetic RNA mimic reduces pain sensitization in mice. Nature Communications, 9(1), 10. 10.1038/s41467-017-02449-5

Bhatt AP, Wong JP, Weinberg MS, Host KM, Giffin LC, Buijnink J, van Dijk E, Izumiya Y, Kung HJ, Temple BRS, & Damania B (2016). A viral kinase mimics S6 kinase to enhance cell proliferation. Proceedings of the National Academy of Sciences of the United States of America, 113(28), 7876–7881. 10.1073/pnas.1600587113 [PubMed: 27342859]

Bhattacharya A, Kaphzan H, Alvarez-Dieppa AC, Murphy JP, Pierre P, & Klann E (2012). Genetic removal of p70 S6 kinase 1 corrects molecular, synaptic, and behavioral phenotypes in fragile X syndrome mice. Neuron, 76(2), 325–337. 10.1016/j.neuron.2012.07.022 [PubMed: 23083736]

Black BJ, Atmaramani R, Kumaraju R, Plagens S, Romero-Ortega M, Dussor G, Price TJ, Campbell ZT, & Pancrazio JJ (2018). Adult mouse sensory neurons on microelectrode arrays exhibit increased spontaneous and stimulus-evoked activity in the presence of interleukin-6. Journal of Neurophysiology, 120, 1374–1385. 10.1152/jn.00158.2018 [PubMed: 29947589]

Black BJ, Atmaramani R, Plagens S, Campbell ZT, Dussor G, Price TJ, & Pancrazio JJ (2019). Emerging neurotechnology for antinoceptive mechanisms and therapeutics discovery. Biosensors & Bioelectronics, 126, 679–689. 10.1016/j.bios.2018.11.015 [PubMed: 30544081]

Bohlen J, & Teleman AA (2021). Phosphorylation of ribosomal protein S6 differentially affects mRNA translation based on ORF length. bio-Rxiv:2021.03.18.436059.

Bolte S, & Cordelières FP (2006). A guided tour into subcellular colocalization analysis in light microscopy. Journal of Microscopy, 224(Pt 3), 213–232. 10.1111/j.1365-2818.2006.01706.x [PubMed: 17210054]

Browne GJ, & Proud CG (2002). Regulation of peptide-chain elongation in mammalian cells. European Journal of Biochemistry, 269(22), 5360–5368. 10.1046/j.1432-1033.2002.03290.x [PubMed: 12423334]

Buritova J, Chapman V, Honore P, & Besson JM (1997). The contribution of peripheral bradykinin B2 receptors to carrageenan-evoked oedema and spinal c-Fos expression in rats. European Journal of Pharmacology, 320(1), 73–80. 10.1016/S0014-2999(96)00872-2 [PubMed: 9049605]

Butler A, Hoffman P, Smibert P, Papalexi E, & Satija R (2018). Integrating single-cell transcriptomic data across different conditions, technologies, and species. Nature Biotechnology, 36(5), 411–420.

Cattaneo A (2010). Tanezumab, a recombinant humanized mAb against nerve growth factor for the treatment of acute and chronic pain. Current Opinion in Molecular Therapeutics, 12(1), 94–106. [PubMed: 20140821]

Chiu R, Boyle WJ, Meek J, Smeal T, Hunter T, & Karin M (1988). The c-Fos protein interacts with c-Jun/AP-1 to stimulate transcription of AP-1 responsive genes. Cell, 54(4), 541–552. 10.1016/0092-8674(88)90076-1 [PubMed: 3135940]

Curtis MJ, Alexander S, Cirino G, Docherty JR, George CH, Giembycz MA, Hoyer D, Insel PA, Izzo AA, Ji Y, MacEwan DJ, Sobey CG, Stanford SC, Teixeira MM, Wonnacott S, & Ahluwalia A (2018). Experimental design and analysis and their reporting II: Updated and simplified guidance for authors and peer reviewers. British Journal of Pharmacology, 175(7), 987–993. 10.1111/bph.14153 [PubMed: 29520785]

Dina OA, Green PG, & Levine JD (2008). Role of interleukin-6 in chronic muscle hyperalgesic priming. Neuroscience, 152(2), 521–525. 10.1016/j.neuroscience.2008.01.006 [PubMed: 18280048]

Dubner R, & Ruda MA (1992). Activity-dependent neuronal plasticity following tissue injury and inflammation. Trends in Neurosciences, 15(3), 96–103. 10.1016/0166-2236(92)90019-5 [PubMed: 1373925]

Ferri GL, Sabani A, Abelli L, Polak JM, Dahl D, & Portier MM (1990). Neuronal intermediate filaments in rat dorsal root ganglia: Differential distribution of peripherin and neurofilament protein immunoreactivity and effect of capsaicin. Brain Research, 515(1–2), 331–335. 10.1016/0006-8993(90)90618-L [PubMed: 2113415]

Gandolfi D, Cerri S, Mapelli J, Polimeni M, Tritto S, Fuzzati-Armentero MT, Bigiani A, Blandini F, Mapelli L, & D'Angelo E (2017). Activation of the CREB/c-Fos pathway during long-term synaptic plasticity in the cerebellum granular layer. Frontiers in Cellular Neuroscience, 11, 184. 10.3389/fncel.2017.00184 [PubMed: 28701927]

Gingras AC, Raught B, & Sonenberg N (2001). Regulation of translation initiation by FRAP/mTOR. Genes & Development, 15(7), 807–826. 10.1101/gad.887201 [PubMed: 11297505]

Gressner AM, & Wool IG (1974). The phosphorylation of liver ribosomal proteins in vivo. Evidence that only a single small subunit protein (S6) is phosphorylated. The Journal of Biological Chemistry., 249(21), 6917–6925. 10.1016/S0021-9258(19)42145-5 [PubMed: 4423396]

Hargreaves K, Dubner R, Brown F, Flores C, & Joris J (1988). A new and sensitive method for measuring thermal nociception in cutaneous hyperalgesia. Pain, 32(1), 77–88. 10.1016/0304-3959(88)90026-7 [PubMed: 3340425]

He Z, Jiang J, Kokkinaki M, Golestaneh N, Hofmann MC, & Dym M (2008). Gdnf upregulates c-Fos transcription via the Ras/Erk1/2 pathway to promote mouse spermatogonial stem cell proliferation. Stem Cells (Dayton, Ohio), 26(1), 266–278.

Hossaini M, Jongen JL, Biesheuvel K, Kuhl D, & Holstege JC (2010). Nociceptive stimulation induces expression of Arc/Arg3.1 in the spinal cord with a preference for neurons containing enkephalin. Molecular Pain, 6, 43. [PubMed: 20653942]

Hunt SP, Pini A, & Evan G (1987). Induction of c-fos-like protein in spinal cord neurons following sensory stimulation. Nature, 328(6131), 632–634. 10.1038/328632a0 [PubMed: 3112583]

Jeevakumar V, Al Sardar AK, Mohamed F, Smithhart CM, & Price T (2020). IL-6 induced upregulation of T-type Ca^{2+} currents and sensitization of DRG nociceptors is attenuated by MNK inhibition. Journal of Neurophysiology, 124(1), 274–283. [PubMed: 32519575]

Kenney JW, Genheden M, Moon KM, Wang X, Foster LJ, & Proud CG (2016). Eukaryotic elongation factor 2 kinase regulates the synthesis of microtubule-related proteins in neurons. Journal of Neurochemistry, 136(2), 276–284. 10.1111/jnc.13407 [PubMed: 26485687]

Knight ZA, Tan K, Birsoy K, Schmidt S, Garrison JL, Wysocki RW, Emiliano A, Ekstrand MI, & Friedman JM (2012). Molecular profiling of activated neurons by phosphorylated ribosome capture. Cell, 151(5), 1126–1137. 10.1016/j.cell.2012.10.039 [PubMed: 23178128]

Krieg J, Hofsteenge J, & Thomas G (1988). Identification of the 40 S ribosomal protein S6 phosphorylation sites induced by cycloheximide. The Journal of Biological Chemistry, 263(23), 11473–11477. 10.1016/S0021-9258(18)37981-X [PubMed: 3403539]

Lewin GR, Rueff A, & Mendell LM (1994). Peripheral and central mechanisms of NGF-induced hyperalgesia. The European Journal of Neuroscience, 6(12), 1903–1912. 10.1111/j.1460-9568.1994.tb00581.x [PubMed: 7704300]

Lilley E, Stanford SC, Kendall DE, Alexander SPH, Cirino G, Docherty JR, George CH, Insel PA, Izzo AA, Ji Y, Panettieri RA, Sobey CG, Stefanska B, Stephens G, Teixeira MM, & Ahluwalia A (2020). ARRIVE 2.0 and the British Journal of Pharmacology: Updated guidance for 2020. British Journal of Pharmacology, 3611–3616. 10.1111/bph.15178 [PubMed: 32662875]

Linderman GC, & Steinerberger S (2019). Clustering with t-SNE, provably. SIAM Journal on Mathematics of Data Science, 1(2), 313–332. 10.1137/18M1216134 [PubMed: 33073204]

Liu D, Stowie A, de Zavalia N, Leise T, Pathak SS, Drewes LR, Davidson AJ, Amir S, Sonenberg N, & Cao R (2018). mTOR signaling in VIP neurons regulates circadian clock synchrony and olfaction. Proceedings of the National Academy of Sciences, 115(14), E3296–E3304.

Mahoney SJ, Dempsey JM, & Blenis J (2009). Cell signaling in protein synthesis ribosome biogenesis and translation initiation and elongation. Progress in Molecular Biology and Translational Science, 90, 53–107. 10.1016/S1877-1173(09)90002-3 [PubMed: 20374739]

Makino H, Seki S, Yahara Y, Shiozawa S, Aikawa Y, Motomura H, Nogami M, Watanabe K, Sainoh T, Ito H, & Tsumaki N (2017). A selective inhibition of c-Fos/activator protein-1 as a potential therapeutic target for intervertebral disc degeneration and associated pain. Scientific Reports, 7(1), 16983. [PubMed: 29208967]

Marvaldi L, Panayotis N, Alber S, Dagan SY, Okladnikov N, Koppel I, Di Pizio A, Song DA, Tzur Y, Terenzio M, & Rishal I (2020). Importin α3 regulates chronic pain pathways in peripheral sensory neurons. Science (New York, NY), 369(6505), 842–846.

Megat S, Ray PR, Moy JK, Lou TF, Barragán-Iglesias P, & Li Y (2019). Nociceptor translational profiling reveals the Ragulator-Rag GTPase complex as a critical generator of neuropathic pain. Journal of Neuroscience, 39(3), 393–411. [PubMed: 30459229]

Melemedjian OK, Asiedu MN, Tillu DV, Peebles KA, Yan J, Ertz N, Dussor GO, & Price TJ (2010). IL-6- and NGF-induced rapid control of protein synthesis and nociceptive plasticity via convergent signaling to the eIF4F complex. The Journal of Neuroscience, 30(45), 15113–15123. 10.1523/JNEUROSCI.3947-10.2010 [PubMed: 21068317]

Melemedjian OK, Khoutorsky A, Sorge RE, Yan J, Asiedu MN, Valdez A, Ghosh S, Dussor G, Mogil JS, Sonenberg N, & Price TJ (2013). mTORC1 inhibition induces pain via IRS-1-dependent

feedback activation of ERK. Pain, 154, 1080–1091. 10.1016/j.pain.2013.03.021 [PubMed: 23607966]

Melemedjian OK, Tillu DV, Moy JK, Asiedu MN, Mandell EK, Ghosh S, Dussor G, & Price TJ (2014). Local translation and retrograde axonal transport of CREB regulates IL-6-induced nociceptive plasticity. Molecular Pain, 10, 1744–8069.

Meyuhas O (2015). Ribosomal protein S6 phosphorylation: Four decades of research. International Review of Cell and Molecular Biology, 320, 41–73. 10.1016/bs.ircmb.2015.07.006 [PubMed: 26614871]

Minatohara K, Akiyoshi M, & Okuno H (2015). Role of immediate-early genes in synaptic plasticity and neuronal ensembles underlying the memory trace. Frontiers in Molecular Neuroscience, 8, 78. [PubMed: 26778955]

Morgan JI, Cohen DR, Hempstead JL, & Curran T (1987). Mapping patterns of c-fos expression in the central nervous system after seizure. Science (New York, NY), 237(4811), 192–197.

Morgan JI, & Curran T (1991). Stimulus-transcription coupling in the nervous system: Involvement of the inducible proto-oncogenes *fos* and *jun*. Annual Review of Neuroscience, 14, 421–451. 10.1146/annurev.ne.14.030191.002225

Moy JK, Khoutorsky A, Asiedu MN, Black BJ, Kuhn JL, Barragan-Iglesias P, Megat S, Burton MD, Burgos-Vega CC, Melemedjian OK, & Boitano S (2017). The MNK-eIF4E signaling axis contributes to injury-induced nociceptive plasticity and the development of chronic pain. The Journal of Neuroscience: The Official Journal of the Society for Neuroscience, 37(31), 7481–7499. 10.1523/JNEUROSCI.0220-17.2017 [PubMed: 28674170]

Nishimoto N, Miyasaka N, Yamamoto K, Kawai S, Takeuchi T, & Azuma J (2009). Long-term safety and efficacy of tocilizumab, an - anti-IL-6 receptor monoclonal antibody, in monotherapy, in patients with rheumatoid arthritis (the STREAM study): Evidence of safety and efficacy in a 5-year extension study. Annals of the Rheumatic Diseases, 68(10), 1580–1584. 10.1136/ard.2008.092866 [PubMed: 19019888]

Oka T, Oka K, Hosoi M, & Hori T (1995). Intracerebroventricular injection of interleukin-6 induces thermal hyperalgesia in rats. Brain Research, 692(1–2), 123–128. 10.1016/0006-8993(95)00691-I [PubMed: 8548295]

Okuzumi T, Fiedler D, Zhang C, Gray DC, Aizenstein B, Hoffman R, & Shokat KM (2009). Inhibitor hijacking of Akt activation. Nature Chemical Biology, 5(7), 484–493. 10.1038/nchembio.183 [PubMed: 19465931]

Park S, Park JM, Kim S, Kim JA, Shepherd JD, Smith-Hicks CL, Chowdhury S, Kaufmann W, Kuhl D, Ryazanov AG, Huganir RL, Linden DJ, & Worley PF (2008). Elongation factor 2 and fragile X mental retardation protein control the dynamic translation of Arc/Arg3.1 essential for mGluR-LTD. Neuron, 59(1), 70–83. 10.1016/j.neuron.2008.05.023 [PubMed: 18614030]

Pearce LR, Alton GR, Richter DT, Kath JC, Lingardo L, Chapman J, Hwang C, & Alessi DR (2010). Characterization of PF-4708671, a novel and highly specific inhibitor of p70 ribosomal S6 kinase (S6K1). The Biochemical Journal, 431(2), 245–255. 10.1042/BJ20101024 [PubMed: 20704563]

Percie du Sert N, Hurst V, Ahluwalia A, Alam S, Avey MT, Baker M, Browne WJ, Clark A, Cuthill IC, Dirnagl U, Emerson M, Garner P, Holgate ST, Howells DW, Karp NA, Lazic SE, Lidster K, MacCallum CJ, Macleod M, … Würbel H (2020). The ARRIVE guidelines 2.0: updated guidelines for reporting animal research. PLoS Biol, 18, e3000410. 10.1371/journal.pbio.3000410 [PubMed: 32663219]

Pirbhoy PS, Farris S, & Steward O (2016). Synaptic activation of ribosomal protein S6 phosphorylation occurs locally in activated dendritic domains. Learning & Memory (Cold Spring Harbor, NY), 23(6), 255–269.

Reichling DB, & Levine JD (2009). Critical role of nociceptor plasticity in chronic pain. Trends in Neurosciences, 32(12), 611–618. 10.1016/j.tins.2009.07.007 [PubMed: 19781793]

Rukwied R, Mayer A, Kluschina O, Obreja O, Schley M, & Schmelz M (2010). NGF induces non-inflammatory localized and lasting mechanical and thermal hypersensitivity in human skin. Pain, 148(3), 407–413. 10.1016/j.pain.2009.11.022 [PubMed: 20022698]

Ruvinsky I, & Meyuhas O (2006). Ribosomal protein S6 phosphorylation: From protein synthesis to cell size. Trends in Biochemical Sciences, 31(6), 342–348. 10.1016/j.tibs.2006.04.003 [PubMed: 16679021]

Ryazanov AG, Shestakova EA, & Natapov PG (1988). Phosphorylation of elongation factor 2 by EF-2 kinase affects rate of translation. Nature, 334(6178), 170–173. 10.1038/334170a0 [PubMed: 3386756]

Sagar SM, Sharp FR, & Curran T (1988). Expression of c-fos protein in brain: Metabolic mapping at the cellular level. Science (New York, NY), 240(4857), 1328–1331.

Sarah Loerch JBDLP, Song J, Pancrazio JJ, Price TJ, & Campbell ZT (2019). Translational controls in pain. In Sossin WS (Ed.), The Oxford handbook of neuronal protein synthesis. Oxford University Press.

Schepetilnikov M, Dimitrova M, Mancera-Martínez E, Geldreich A, Keller M, & Ryabova LA (2013). TOR and S6K1 promote translation reinitiation of uORF-containing mRNAs via phosphorylation of eIF3h. The EMBO Journal, 32(8), 1087–1102. 10.1038/emboj.2013.61 [PubMed: 23524850]

Sonenberg N, & Hinnebusch AG (2009). Regulation of translation initiation in eukaryotes: Mechanisms and biological targets. Cell, 136(4), 731–745. 10.1016/j.cell.2009.01.042 [PubMed: 19239892]

Usoskin D, Furlan A, Islam S, Abdo H, Lonnerberg P, Lou D, Hjerling-Leffler J, Haeggström J, Kharchenko O, Kharchenko PV, & Linnarsson S (2015). Unbiased classification of sensory neuron types by large-scale single-cell RNA sequencing. Nature Neuroscience, 18(1), 145–153. 10.1038/nn.3881 [PubMed: 25420068]

Wool IG, Chan YL, & Glück A (1995). Structure and evolution of mammalian ribosomal proteins. Biochimie et Biologie Cellulaire, 73(11–12), 933–947. 10.1139/o95-101 [PubMed: 8722009]

Yanagiya A, Suyama E, Adachi H, Svitkin YV, Aza-Blanc P, Imataka H, Mikami S, Martineau Y, Ronai Z'A, & Sonenberg N (2012). Translational homeostasis via the mRNA cap-binding protein, eIF4E. Molecular Cell, 46(6), 847–858. 10.1016/j.molcel.2012.04.004 [PubMed: 22578813]

Zachariou V, Bolanos CA, Selley DE, Theobald D, Cassidy MP, Kelz MB, Shaw-Lutchman T, Berton O, Sim-Selley LJ, Dileone RJ, Kumar A, & Nestler EJ (2006). An essential role for DeltaFosB in the nucleus accumbens in morphine action. Nature Neuroscience, 9(2), 205–211. 10.1038/nn1636 [PubMed: 16415864]

What is already known about this subject

- Translational control in nociceptors plays an integral role in chronic pain.
- c-Fos is important in the development and maintenance of neuropathic pain.

What does this study adds

- S6K1 regulates preferential translation of c-Fos in DRG neurons after treatment of inflammatory mediators.
- Pharmacological inhibition of S6K1 (DG2) or c-Fos (T-5224) blocks inflammation-related neuronal firing and behavioural hypersensitivity.

What is the clinical significance

- We identified the S6 kinase pathway as a novel target for pain.
- The low MW inhibitors DG2 and T-5224 may function as broad-spectrum antihyperalgesics.

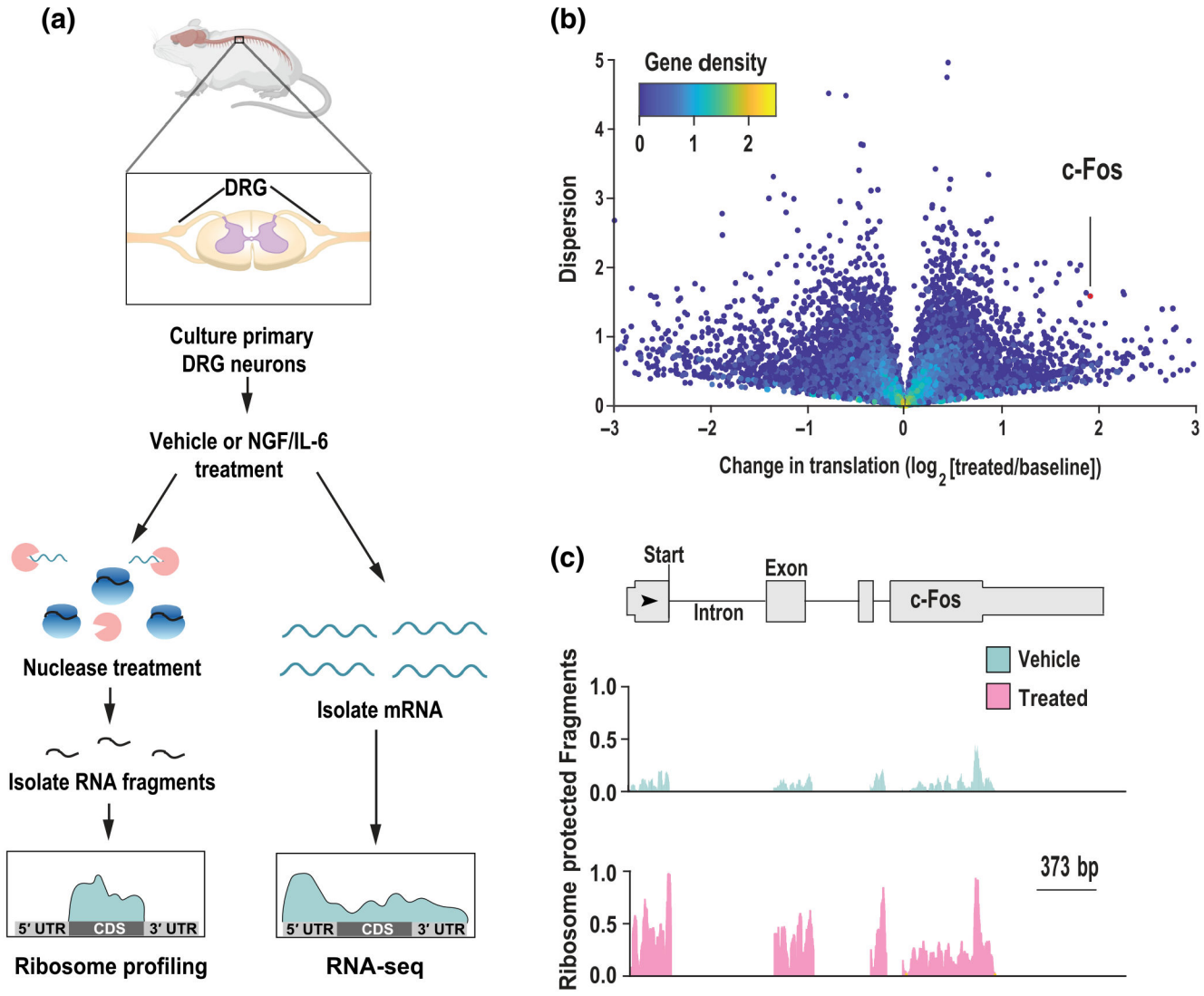

FIGURE 1.

Ribosome profiling reveals c-Fos as a target of preferential translation. (a) Schematic representation of ribosome profiling in cultured DRG neurons. Cultures were generated from DRG tissues prior to treatment with inflammatory mediators. After brief exposure to NGF and IL-6, translation was arrested with the addition of emetine. Lysates were subjected to limited RNAse digestion, and the resulting footprints were isolated and sequenced. RNA-seq was performed in parallel. (b) A volcano plot showing changes in translation ($\log_2 \geq -1.5$; false discovery rate < 0.05). The ratio of ribosome density following treatment with NGF/IL-6 divided by the vehicle levels is plotted against sample dispersion. Gene density is shaded according to the inset bar. The *P* value for c-Fos (0.028) was determined using a two-tailed Student's *t* test. (c) Traces of ribosome protected footprints on the c-Fos gene with vehicle or NGF/IL-6 treatment. The vehicle group (blue) is shown above the NGF- and IL-6-treated group (pink)

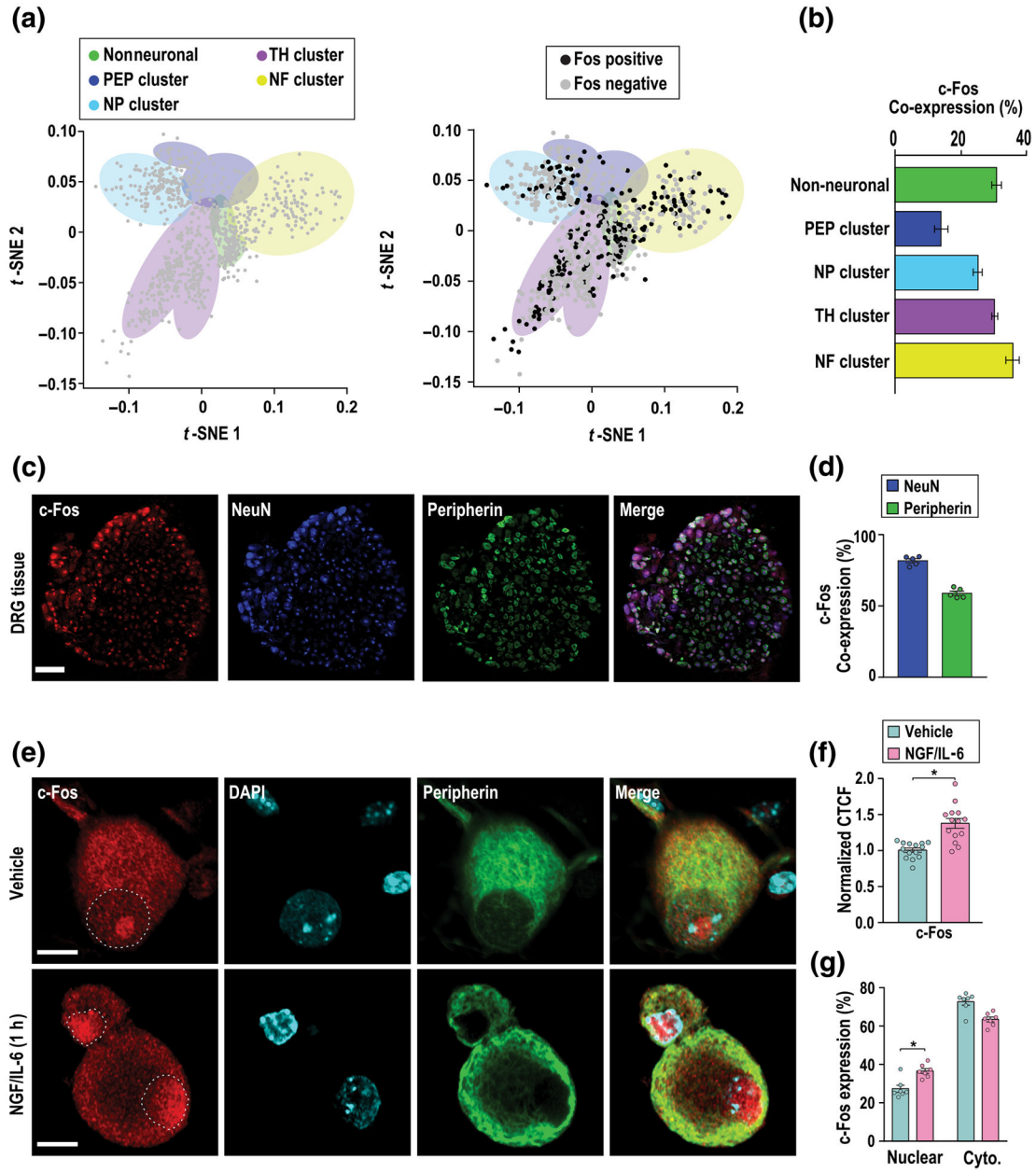

FIGURE 2.

c-Fos is expressed in DRG neurons. (a) Single-cell clusters based on the expression of marker genes for the following populations of cells: non-neuronal (*Vim*), peptidergic (PEP; *Calca/CGRP*), non-peptidergic (NP; *Mrgprd*), tyrosine hydroxylase (TH; *Th*) and a neurofilament present in large-diameter neurons (*Nefh*). Data were obtained from Usoskin et al. (2015) and subjected to unbiased clustering. Right—Cells that express c-Fos are shaded in black, whereas the c-Fos negative cells are shown in grey in the clusters defined by marker gene expression. (b) Quantification of co-expression of c-Fos with marker genes. c-Fos is ubiquitously expressed in non-neuronal and neuronal cells. There is no significant difference in c-Fos co-expression between neuronal and non-neuronal cell categories. (c) IHC demonstrated that c-Fos (red) is broadly expressed in DRG neurons and co-localizes

with NeuN (blue), a pan-neuronal marker, and peripherin (green), a marker for nociceptive neurons. Scale bar = 100 μm. (d) Quantification of co-expression of c-Fos with NeuN (blue) and peripherin (green). $n = 5$ DRGs from three different animals. (e) Representative ICC images from primary DRG cultures showing c-Fos expression after treatment with vehicle or NGF/IL-6. Representative images of cells labelled for c-Fos (red), peripherin (green) and the nuclear marker DAPI (cyan). Scale bar = 10 μm. (f) Quantification of ICC images comparing c-Fos levels between untreated and NGF/IL-6-treated peripherin-positive DRG neurons. $*P < 0.05$, significantly different as indicated; unpaired Student's *t*-test. Data presented are individual values with means ± SEM; $n = 14$ cells per group. (g) Analysis of c-Fos localization. Treatment of NGF/IL-6 also increased nuclear localization of c-Fos. Ratio of c-Fos expression in the nucleus to that in cytoplasm after vehicle or NGF/IL-6 treatment. $*P < 0.05$, significantly different as indicated; unpaired Student's *t*-test. Data are presented as individual values with means ± SEM; $n = 7$ cells per group

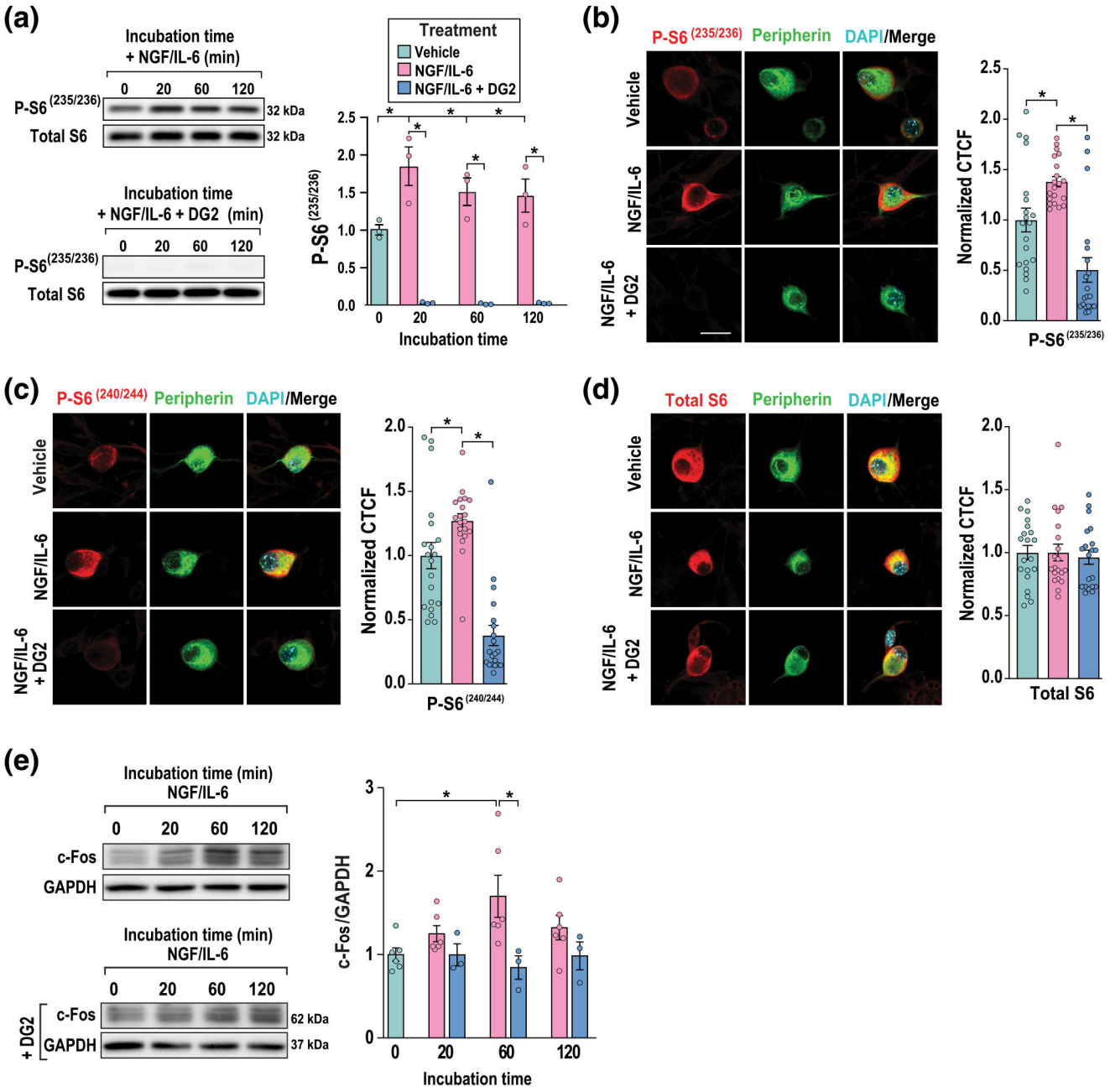

FIGURE 3.

S6K1 mediates translation of c-Fos. (a) Treatment of primary DRG cultures with NGF/IL-6 increased phosphorylation of S6 at the $S^{235/236}$ position, whereas total S6 levels were unchanged. This NGF/IL-6-induced phosphorylation was abolished by co-treatment with the S6K1 inhibitor DG2 (20 μM). Data presented are individual values with means; $n = 3$ samples per group. $*P < 0.05$, significantly different as indicated; $F_{(1,4)} = 54.36$, two-way ANOVA with Sidak's multiple comparisons test. (b) ICC images from primary DRG cultures showing increased phosphorylation of S6 at the $S^{235/236}$ position with NGF/IL-6 treatment, which was blocked by co-treatment of DG2. Data presented are individual values with means ± SEM; $n = 20$ cells per group. $*P < 0.05$, significantly different as indicated; $F_{(2,57)}$

= 18.48, one-way ANOVA with Sidak's multiple comparisons test. (c) Treatment of NGF/IL-6 on primary DRG cultures increased phosphorylation of S6 at the $S^{240/244}$ position, which was abolished by co-treatment with DG2. Data presented are individual values with means ± SEM; $n = 20$ cells per group. $^{*}P < 0.05$, significantly different as indicated; $F_{(2,57)} = 36.10$, one-way ANOVA with Sidak's multiple comparisons test. (d) ICC images showing no change in the levels of total S6. Data presented are individual values with means ± SEM; $n = 20$ cells per group. (e) S6K1 activity is required for translational stimulation of c-Fos triggered by NGF/IL-6. DG2 blocked preferential translation of c-Fos, but it had no effect on the production of the GAPDH control. Data presented are individual values with means ± SEM; $n = 6$ for the vehicle and NGF/IL-6 group, $n = 3$ for the NGF/IL-6 + DG2 group. $^{*}P < 0.05$, significantly different as indicated; $F_{(1,10)} = 5.509$, two-way ANOVA with Sidak's multiple comparisons test. Full blots are presented in Figure S2

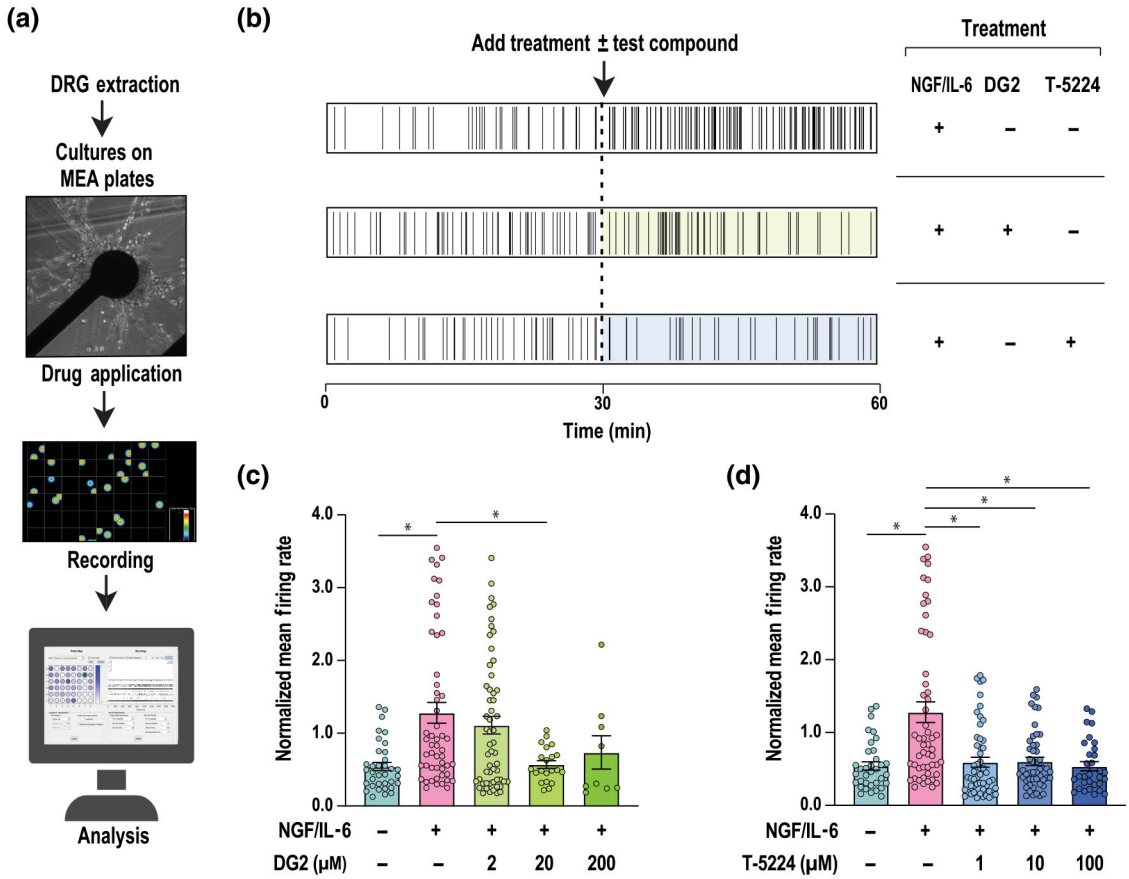

FIGURE 4.

Pharmacological inhibition of S6K1 or c-Fos blocks NGF/IL-6-evoked sensory neuron excitability. (a) A schematic of the multielectrode array (MEA) approach. DRG neurons are cultured on plates containing electrodes. Baseline levels of activity were first assessed, and then, treatments were added to the culture media of each well. All data are stored and processed using computers with the Axion Maestro software. (b) Raster plots showing representative recordings for baseline and drug treatment over a 30-min period. A 30-min baseline is shown prior to the addition of NGF and IL-6 along with the compounds indicated on the left. (c) DG2 (20 μM) blocked NGF/IL-6-evoked neuronal firing rates. Data presented are individual values with means ± SEM; $n = 35$ (vehicle), 53 (NGF/IL-6), 56 (NGF/IL-6 + 2 μM DG2), 21 (NGF/IL-6 + 2 μM DG2) and 9 (NGF/IL-6 + 200 μM DG2). *$P < 0.05$, significantly different as indicated; $F_{(4,169)} = 6.394$, One-way ANOVA with Sidak's multiple comparisons test. (d) The c-Fos inhibitor, T-5224, diminished NGF/IL-6-induced firing. Data presented are individual values with means ± SEM; $n = 35$ (vehicle), 53 (NGF/IL-6), 52 (NGF/IL-6 + 1 μM T-5224), 49 (NGF/IL-6 + 1 μM T-5224) and 31 (NGF/IL-6 + 1 μM T-5224). *$P < 0.05$, significantly different as indicated; $F_{(4,215)} = 13.02$, one-way ANOVA with Sidak's multiple comparisons test

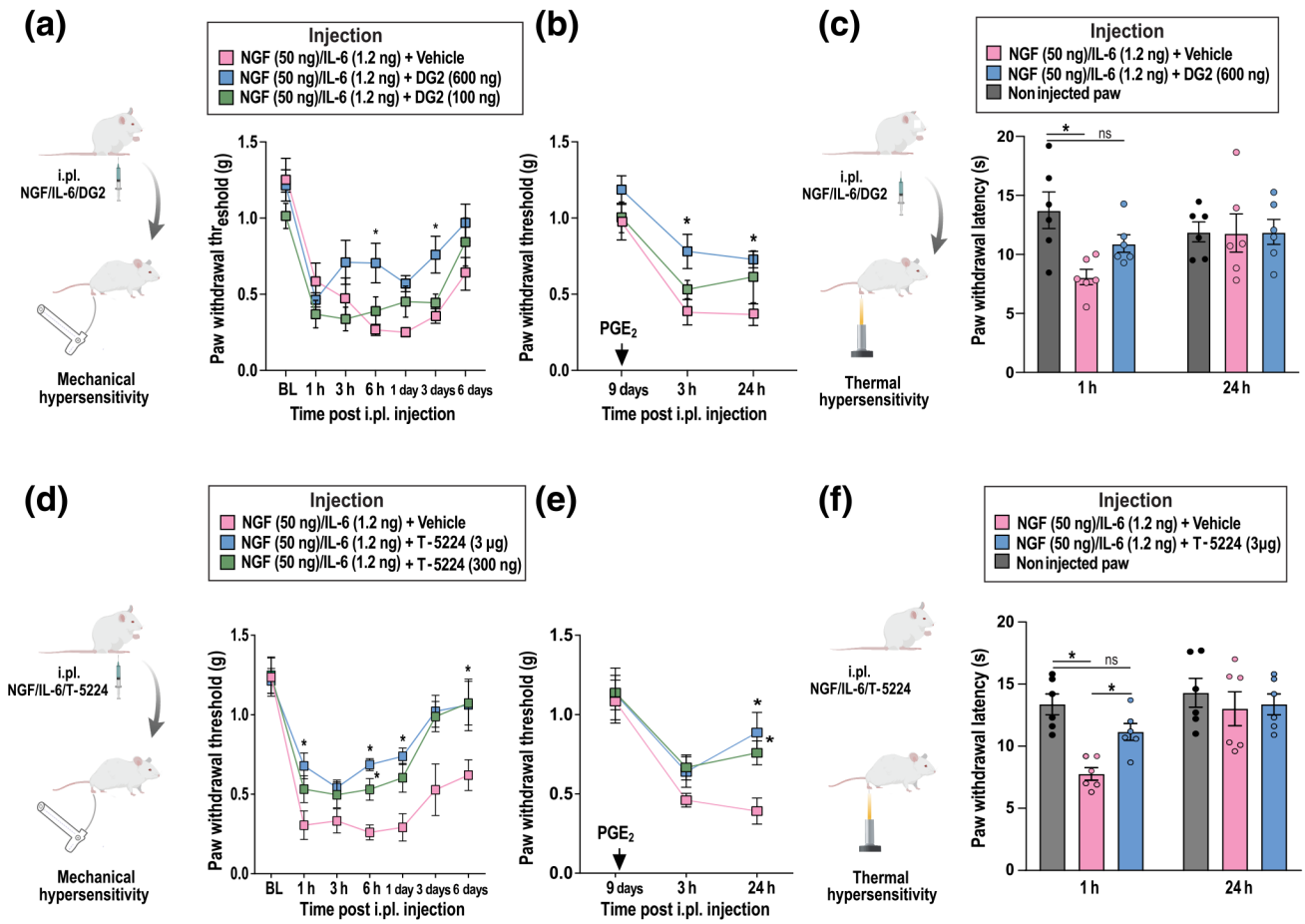

FIGURE 5.

DG2 and T-5224 ameliorate NGF/IL-6-induced mechanical and thermal hypersensitivity. (a) Intraplantar (i.pl.) injection of NGF/IL-6 decreased the withdrawal threshold of mice to calibrated von Frey filaments, indicating mechanical hypersensitivity. This mechanical hypersensitivity induced by NGF/IL-6 was attenuated by co-treatment with the high dose (600 ng), but not of the low dose (100 ng), of DG2. Data are presented as means ± SEM; n = 6 animals per group. *P < 0.05, significant effect of DG2; drug effect, $F_{(2,21)}$ = 6.865, two-way ANOVA with Sidak's multiple comparisons test. (b) Following resolution of the acute mechanical hypersensitivity, at Day 9, mice were given a subthreshold dose of PGE_2 (100 ng, i.pl.). Mice treated with NGF/IL-6 exhibited reduced withdrawal threshold indicating the development of hyperalgesic priming. Mice that were co-injected with 600 ng of DG2, but not the 100-ng dose, showed ameliorated response to PGE_2. Data are presented as means ± SEM; n = 6 animals per group. *P < 0.05, significant effect of DG2; drug effect, $F_{(2,21)}$ = 8.531, two-way ANOVA with Sidak's multiple comparisons test. (c) NGF/IL-6 transiently reduced withdrawal latency upon application of a radiant heat source (Hargreave's method), indicating thermal hypersensitivity. DG2 (600 ng) ameliorated the thermal hypersensitivity caused by NGF/IL-6 treatment. Data presented are individual values with means ± SEM; n = 6 animals per group. *P < 0.05, significantly different as indicated; drug effect, $F_{(2,30)}$ = 3.346, two-way ANOVA with Sidak's multiple comparison test. ns = not significant. (d) The c-Fos inhibitor, T-5224, reduced NGF/IL-6-induced mechanical hypersensitivity in the

von Frey test. Data are presented as mean ± SEM; $n = 6$ animals per group. *$P < 0.05$, significant effect of T-5224; drug effect, $F_{(2,15)} = 20.16$, two-way ANOVA with Sidak's multiple comparisons test. (e) Hyperalgesic priming to PGE2 was also reduced in T-5224 treated mice. Data are presented as mean ± SEM; $n = 6$ animals per group. *$P < 0.05$, significant effect of T-5224; time effect, $F_{(2,30)} = 29.40$, two-way ANOVA with Sidak's multiple comparisons test. (f) T-5224 also attenuated the thermal hypersensitivity produced by NGF/IL-6. Data presented are individual values with means ± SEM; $n = 6$ animals per group. *$P < 0.05$, significantly different as indicated; drug effect, $F_{(2,30)} = 6.669$, two-way ANOVA with Sidak's multiple comparisons test. ns = not significant

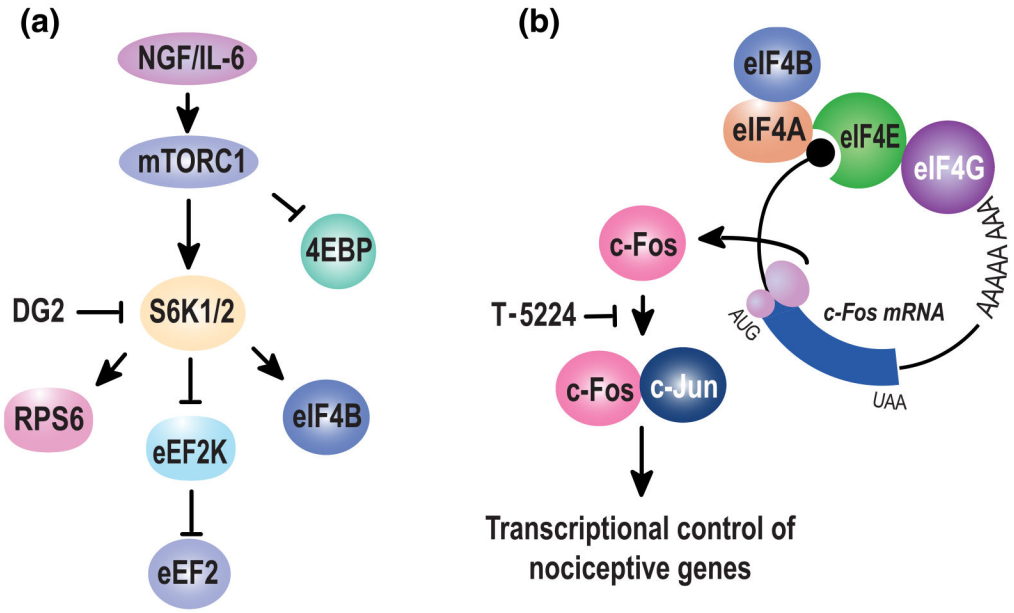

FIGURE 6.

A model for translational regulation of c-Fos. (a) NGF and IL-6 stimulate mTOR which acts on both 4EBPs and S6Ks. Downstream of S6Ks are three main effectors, the ribosomal protein S6, eEF2K and eIF4B. It is unclear which pathway is responsible for induction of c-Fos. (b) Translation is potentially regulated at multiple points through S6Ks. For example, eIF4B stimulates eIF4A, and although the precise function of S6 phosphorylation is not known, S6 is a component of the 40S ribosome (Ruvinsky & Meyuhas, 2006). eEF2 phosphorylation inactivates translation although the precise molecular mechanism is not clear (Ryazanov et al., 1988). Once translated, c-Fos forms heterodimers with c-Jun, and we propose that the complex regulates nociceptive transcriptional networks (Chiu et al., 1988)